Structural characterization of 9-cyanoanthracene–water by rotational coherence spectroscopy

ARTICLE *in* CHEMICAL PHYSICS LETTERS · FEBRUARY 2001

Impact Factor: 1.9 · DOI: 10.1016/S0009-2614(00)01446-9

3 AUTHORS, INCLUDING:

Kazuhiro Egashira
Genesis Research Institute, Inc.
18 PUBLICATIONS **232** CITATIONS
SEE PROFILE

Yasuhiro Ohshima
Institute for Molecular Science
110 PUBLICATIONS **2,204** CITATIONS
SEE PROFILE

9 February 2001

ELSEVIER

Chemical Physics Letters 334 (2001) 285–292

CHEMICAL PHYSICS LETTERS

www.elsevier.nl/locate/cplett

Structural characterization of 9-cyanoanthracene–water by rotational coherence spectroscopy

Kazuhiro Egashira [a], Yasuhiro Ohshima [a,*], Okitsugu Kajimoto [a,b]

[a] *Department of Chemistry, Graduate School of Science, Kyoto University, Kitashirakawa-Oiwakecho, Sakyo-ku, Kyoto 606-8502, Japan*
[b] *Core Research for Evolutional Science and Technology (CREST), Japan Science and Technology Corporation (JST), Honcho u-chome, Kawaguchi City, Saitama Pref. 332-0012, Japan*

Received 30 October 2000; in final form 4 December 2000

Abstract

Rotational coherence spectroscopy (RCS) has been applied to determine the rotational constants of the two isotopic species of the 9-cyanoanthracene (CNA)–water complex, CNA–H_2O, and CNA–D_2O. To support the experimental observation, DFT calculations at the B3LYP/6-31G(d, p) level have been also performed to identify several stable conformations. The structure of the complex is found to be such that water is hydrogen-bonded to the π-electrons of the cyano group of CNA. Geometrical parameters consistent with the experimental results are evaluated.

1. Introduction

Hydrogen bonds are of fundamental importance in various processes of chemistry and biology. Spectroscopic studies of weakly bound molecular complexes formed in supersonic expansions have provided a wealth of information on the structures and dynamics of such species and defined the starting point for detailed understanding on hydrogen bonding. In particular, hydrated complexes of an aromatic molecule with a polar functional group have been extensively studied with motivation for modeling solvation processes and possible influence of hydrogen bonding on charge-transfer reactions. As a model for microscopic solvation, aromatic molecules with a cyano group have unique characteristics, because they have three possible hydrogen-accepting sites: (1) the triple bond of the CN group; (2) the nitrogen atom of the CN group having non-bonding electrons; and (3) the π-electrons of the aromatic moiety. Furthermore, some of these complexes are well known as electron acceptors or molecules which undergo twisted intramolecular charge-transfer reactions. Many spectroscopic studies on 1:1 hydrated complexes have so far been reported for aromatic molecules with cyano groups, e.g., benzonitrile [1–7], 4-aminobenzonitrile [8], 4-(*N*, *N*-dimethylamino)benzonitrileDMABN) [9–13], 4-pyrrolidinobenzonitrile [14], *p*-dicyanobenzene [15], 1-cyanonaphthalene [16], and 9-cyanoanthracene (CNA) [17]. Among them benzonitrile–water has been studied most extensively in its ground and excited electronic states with various spectroscopic methods such as rotational contour analysis [1], Fourier-transform microwave (FTMW) spectroscopy [2–4,6],

* Corresponding author. Fax: +81-75-753-3974.
E-mail address: ohshima@kuchem.kyoto-u.ac.jp (Y. Ohshima).

0009-2614/01/$ - see front matter
PII: S0009-2614(00)01446-9

high-resolution UV spectroscopy [3], and stimulated Raman– and IR–UV double resonance spectroscopy [5,7]. Accordingly, it has been well established that this complex has a planar structure in which water is hydrogen-bonded perpendicularly to the CN group [2–4,6]. However, structural information on other hydrated complexes is much less abundant. For instance, no experimental data have been reported on complexes involving larger aromatic molecules. Structural implication of 1-cyanonaphthalene–water was based on calculations of an empirical model potential [16], which has to be experimentally confirmed. Though the LIF spectrum was measured for CNA–water [17], there has been no discussion on its structure.

In this Letter, we report rotational coherence spectroscopy (RCS) on two isotopomers of the CNA complex with water, i.e., CNA–H_2O and CNA–D_2O. Expansion of the aromatic moiety from phenyl (such as benzonitrile) to anthryl (CNA) could make the dispersive interaction more important. RCS is particularly valuable as a spectroscopic method with rotational resolution for structural studies of large gas-phase species [18]. For instance, we have already reported a structural study of CNA–$(Ar)_n$ ($n = 1$–3) clusters by RCS to confirm that these clusters are of wet type, in which Ar atoms reside on both sides of the CNA aromatic plane for $n \geqslant 2$ [19]. The present RCS results allow us to determine the rotational constants of CNA–water, and accordingly the structural parameters relating to the hydrogen bonding in it. The derived parameters are compared with those in the minimum-energy structures obtained from molecular orbital (MO) calculations.

2. Experimental

2.1. RCS measurements

Details of the present experimental setup have been described elsewhere [19]. The RCS experiments were performed by utilizing time-resolved fluorescence depletion (TRFD) [20,21] with a solid-state picosecond laser system. It is composed of a femtosecond mode-locked Ti:sapphire laser (Spectra Physics, Tsunami) pumped by a diode-pumped cw Nd:YVO_4 laser (Spectra Physics, Millennia) and a picosecond regenerative amplifier (Spectra Physics, Spitfire) pumped by a Q-switched Nd:YLF laser (Spectra Physics, Merlin). The amplified output was 0.5 mJ per pulse at a repetition rate of 1 kHz, with a pulse width of ≈1 ps (fwhm) and the bandwidth below 1 nm. The fundamental of the ps laser radiation was frequency-doubled in an $LiBO_3$ crystal to produce excitation pulses for transitions of the species to be studied. The second harmonic thus generated was directed thorough a Michelson interferometer to generate the pump and variably delayed probe pulses of equal intensity. The pump and probe pulse trains, polarized parallel to one another, were recombined and sent collinearly into a vacuum chamber after collimation to ≈1 mm diameter. The pulse trains intersected supersonic free jets perpendicularly at a distance of 5 mm from the expansion orifice. The averaged output of the UV light was ≈50 μJ/pulse, and its spectral bandwidth was ≈0.2 nm in the UV region.

The 1:1 complex of CNA with water was formed in supersonic free-jet expansions. CNA was vaporized in a sample reservoir directly attached to a cw nozzle, both being heated to about 150°C by a sheath heater. The carrier gas, primarily of helium with a small amount of H_2O (distilled water) or D_2O (Euriso-top; 99.8% isotopic purity), was mixed at room temperature by means of a needle-valve arrangement. It was regulated to be 5 atm and led into the reservoir of CNA. The gas sample containing a trace amount of vaporized CNA was expanded continuously into a vacuum chamber through a small orifice (70 μm in diameter). The pressure in the chamber was maintained at 5×10^{-4} Torr during the experiment.

Time-integrated fluorescence was collected using two quartz lenses, filtered with a sharp-cut long-pass filter to eliminate scattered light from the excitation pulse, and detected with a photomultiplier tube held perpendicularly to the laser and molecular beams. The fluorescence signal was preamplified, filtered by a 1-kHz high-pass filter, and fed into a boxcar integrator, whose output

was finally stored by a personal computer as a function of the delay between the pump and probe pulses to yield a TRFD trace. A typical completed scan corresponds to an average of some dozens of individual traces, each obtained by averaging 300 laser shots at each delay position.

Before the RCS measurements, laser-induced fluorescence (LIF) spectra of the CNA complex with water were observed using a dye laser (Lambda Physik, SCANmate 2E) pumped by a 10-Hz XeCl excimer laser (Lambda Physik, COMPex 102) to determine the transition frequency of each species and optimize the conditions. The UV light (bandwidth <0.5 cm^{-1}) crossed the molecular jet 5 mm downstream of the cw nozzle. Fluorescence was detected and averaged with the apparatus used in the TRFD experiments.

2.2. Molecular orbital calculations

MO calculations were performed to obtain minimum-energy structures of the CNA–H_2O complex in the electronic ground state. First, a number of structural optimizations at the RHF/6-31G level were carried out for various relative configurations of water molecule. The stable structures thus identified by these global surveys were further optimized by DFT calculations using the Becke3LYP functional with a 6-31G(d, p) basis set. Normal - mode vibrational analyses were performed for such optimized structures to ensure that they represented true potential minima. The standard counterpoise procedure was used for corrections of the basis set superposition error (BSSE) in the binding energies. Corrections for the zero-point vibrational energy were also included. All the calculations were carried out using the GAUSSIAN98 program package [22] on a personal computer.

3. Results

3.1. LIF measurements

Fig. 1 shows the LIF spectrum of the CNA cluster with H_2O in the region of 382–388 nm. The spectrum is essentially the same as that reported in

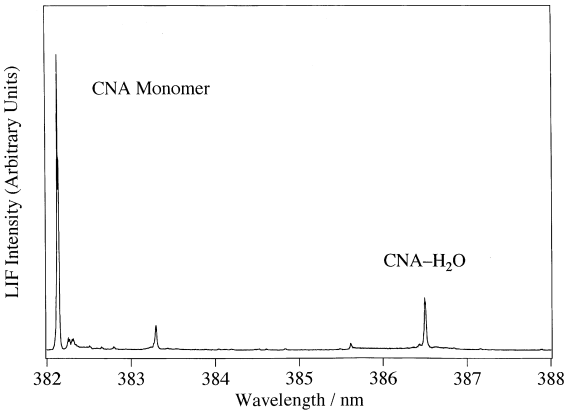

Fig. 1. LIF spectrum of CNA–H_2O formed under the jet-cooled condition.

[17]. The large peak at 382.13 nm (in air) has been assigned to the electronic origin of the CNA monomer [23]. The band at 386.50 nm, with a shift ($\delta\nu$) of -296 cm^{-1} from the 0_0^0 band of bare CNA, is assigned to the electronic origin of the CNA–H_2O complex. In addition, the band at 383.29 nm is assigned to a vibronic band of the complex, which is correlated to an intramolecular low-frequency mode of CNA with vibrational excess energy of 217 cm^{-1} [23]. There appear no prominent vibronic bands involving intermolecular modes, which suggests that a structural change of this complex caused by the electronic excitation is small. It is also noted that there is no indication of other isometric form(s) with comparable intensity. The LIF spectrum for CNA–D_2O is similar to that in Fig. 1, where the band origin of the complex is located at $\delta\nu = -301$ cm^{-1}.

3.2. RCS measurements

Fig. 2a shows an RCS–TRFD trace measured by monitoring the S_1–S_0 0_0^0 band of CNA–H_2O at $\delta\nu = -296$ cm^{-1}. A raw trace showed an almost linearly changing baseline due to delay dependence in the background fluorescence levels caused by lifetime effects [20], delay-line misalignment, laser beam divergence, etc., and thus the trace shown in Fig. 2a was subjected to baseline subtraction. Two sets of transients are visible in the trace. The transients in one set (marked with C's), spaced by

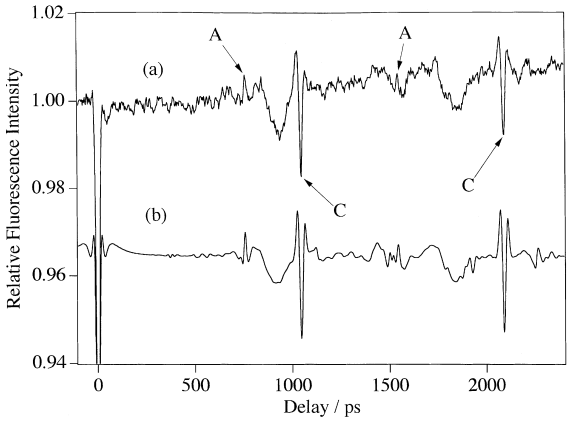

Fig. 2. RCS traces of CNA–H_2O. (a) Experimental TRFD trace recorded with the band at $\delta\nu = -296$ cm^{-1}. Features labeled with C's (A's) have been assigned to the *C*-type (*A*-type) rotational coherence transients. (b) Simulated trace which reproduces the experimental trace the best. The rotational constants for the calculated trace were taken as 0.664, 0.373, and 0.239 GHz for *A*, *B* and *C*, respectively. The ratio of the *a*-, *b*-, and *c*-axis components of the transition dipole is 0.395:0.919:0.0. The horizontal scale indicates the relative intensity for the observed fluorescence, and the calculated trace is scaled to fit to the experimental one.

1044 ps, appear at $t \approx n/(4C)$ (n being an integer) with negative polarity throughout the trace. The transients in the second set (marked with A's) appear weakly at $t \approx n/(4A)$ (only even n being prominent) with positive polarity. The trace obtained for CNA–D_2O exhibits analogous features.

The RCS traces so obtained were compared with simulated ones to estimate the rotational constants from the data. Simulations were carried out by using a program, coded in accord with the theoretical scheme by Felker et al. [24–26]. For simplicity, the ground state expression for RCS transients was employed [26]. In performing the simulations the rotational temperature was assumed to be 5 K, for which the widths of the observed transients were well reproduced. Since the laser pulse duration was much narrower than the TRFD transients, no convolution was necessary for simulating the RCS traces. The *A* and *C* constants thus estimated for CNA–H_2O and CNA–D_2O are listed in Table 1. The widths of the *A*- and *C*-type transients are ≈20 ps (fwhm), which set the uncertainties in the listed rotational constants (≤0.5%).

Table 1
RCS-derived rotational constants of CNA–H_2O and CNA–D_2O (in GHz)[a]

	A	*C*
CNA–H_2O	0.664	0.239
CNA–D_2O	0.647	0.233

[a] Estimated uncertainties are ±0.5%.

3.3. Molecular orbital calculations

MO calculations were performed to predict the most probable isomer that reproduced the experimental trace. Three minimum-energy structures were obtained by geometry optimization at the DFT/B3LYP/6-31G(d, p) level. They are labeled in Figs. 3a–c, as side-, linear-, and opposite-type, respectively. Calculated binding energies of the three isomers are listed in Table 2. The structure of the side-type isomer is such that the water molecule is hydrogen-bonded as a proton donor to the triple bond of the cyano group of CNA and also hydrogen-bonded as a proton acceptor to the 1-position hydrogen atom of CNA. In the linear-type isomer, however, water is attached as a proton donor to the lone pair of the nitrogen atom. In both cases the molecular plane of water is almost perpendicular to that of CNA. The water molecule in the opposite-type isomer is hydrogen-bonded as a proton acceptor to the 10-position hydrogen of CNA; this structure has C_s symmetry. The π-type isomer, where water lies on the CNA plane, was not identified as a local minimum at the present level of calculations despite our careful search. On the other hand, this type has been predicted to be stable for DMABN–H_2O by the SCF–MO CI calculations [27]. The present calculations also predicted that such a conformation is unstable in which the water molecule is hydrogen-bonded to the triple bond of the CN group and the OH bond involved in the hydrogen bond is perpendicular to the CNA plane.

The opposite-type is much less stable than the other two configurations, as shown in Table 2. In particular, its binding energy is quite small when the BSSE correction is included. On the contrary, the side-type and linear-type isomers are much more stable. Their binding energies are so close that they are reversed whether or not the BSSE

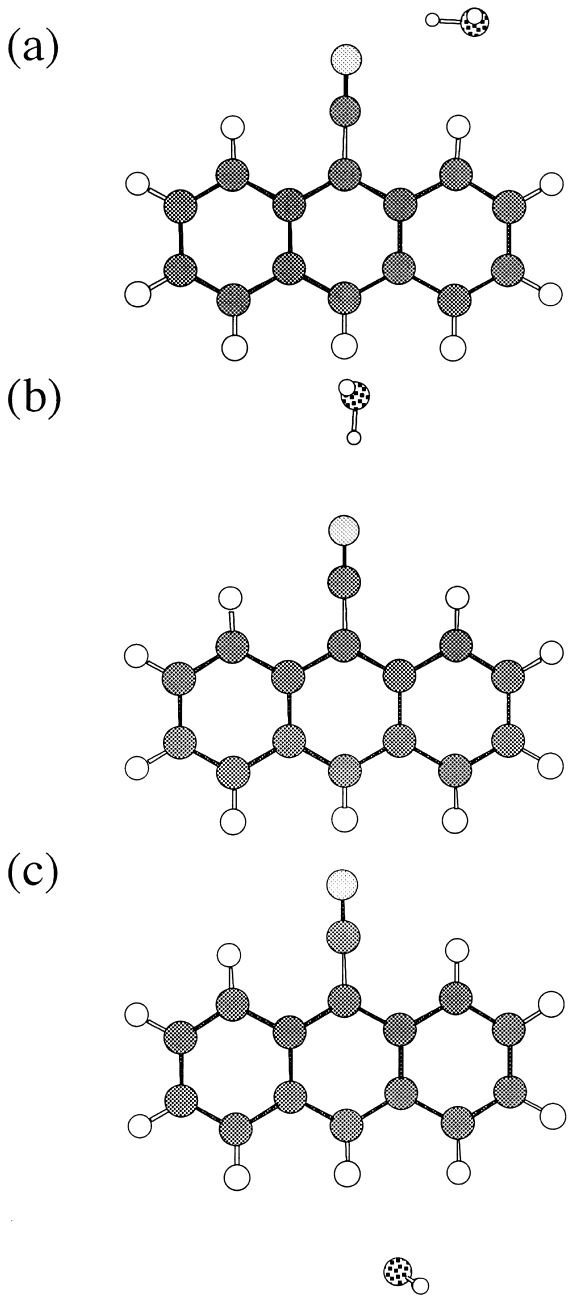

Fig. 3. Geometries of CNA–H_2O isomers obtained from DFT/B3LYP/6-31G(d, p) calculations. (a) Side-type. (b) Linear-type. (c) Opposite-type.

correction is considered. Therefore, we cannot say at the present stage which could be the global minimum of CNA–H_2O.

These two types of local minima have been predicted for benzonitrile–water complexes; calculations at the RHF/6-31G(d, p) level identified two stable structures, where the side-type was 0.62 kcal/mol more stable than the linear-type [5]. This is also the case for 1-cyanonaphthalene–water, where the side-type was calculated by the exchange perturbation method to be 0.15 kcal/mol more stable [16].

4. Analysis of structures

In this section we use the RCS results reported above to determine the zero-point geometrical parameters for the CNA–water complex. In doing this we make the usual assumptions that the geometries of the CNA molecule [19] and water [28] do not change upon complexation and that isotopic substitution has no effect on the structures of the complexes. Note that in this work the observed rotational coherence effects represent the unresolved contributions of ground- and excited-state coherences [25]. Therefore, the structural parameters derived from the present RCS–TRFD data represent averages of the parameters in the two states. In other words, they are identical for S_1 and S_0 within the quoted uncertainties. This is in accord with the above-mentioned negligible Franck–Condon activity for intermolecular vibrations in the observed LIF spectrum, which implies the smallness of the structural change after photoexcitation.

To study the gross geometry of the complex, we first compare the experimental trace with simulated traces for the isomers identified by the above-mentioned DFT calculations, shown in Fig. 4. In these simulations the transition dipole is assumed to be parallel to the in-plane short axis of the CNA moiety [29]. A comparison of the experimental and simulated traces rules out the linear-type isomer, primarily due to the difference in positions of the *C*-type transients. The opposite-type gives the *C*-type transients that are close in position to the observed ones. However, it lacks the weak *A*-type transients that are present in the measured trace. The simulated trace for the side-type isomer, on the other hand, matches all aspects of the

Table 2
Calculated binding energies and rotational constants of the CNA–H_2O isomers[a]

	ΔE^{Nb}	ΔE^{Bc}	A^d	B^d	C^d
Side-type	5.88	2.64	0.6702	0.3755	0.2409
Linear-type	4.14	3.07	0.4514	0.4087	0.2147
Opposite-type	3.30	0.77	0.5539	0.4260	0.2411

[a] Obtained by DFT/B3LYP/6-31G(d, p) calculations.
[b] Binding energy (in kcal/mol) without BSSE correction.
[c] Binding energy (in kcal/mol) with BSSE correction.
[d] In GHz.

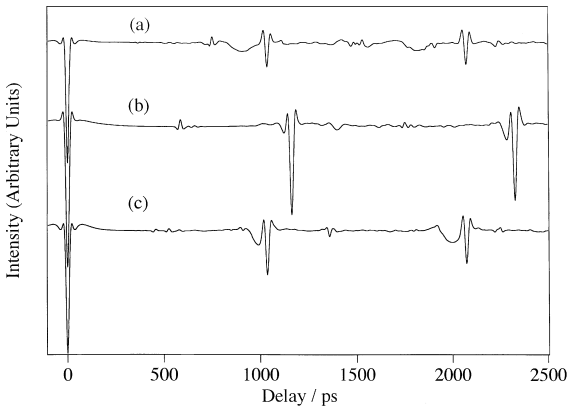

Fig. 4. Simulated RCS traces of CNA–H_2O isomers obtained from DFT calculations. Rotational constants used are listed in Table 2. (a) Side-type. The ratio of the *a*-, *b*-, and *c*-axis components of the transition dipole is 0.3836:0.9234:0.0127. (b) Linear-type. The ratio of the *a*-, *b*-, and *c*-axis components of the transition dipole is 0.9692:0.2459:0.0144. (c) Opposite-type. The ratio of the *a*-, *b*-, and *c*-axis components of the transition dipole is 0.3860:0.9225:0.0000.

experimental results quite well, including broad transients which do not correspond to any of *J*-, *K*-, *A*-, or *C*-type recurrence. Thus, the gross structure of the CNA–water complex was determined to be of side-type.

For further consideration, a least-squares fitting was performed to estimate geometrical parameters. In general, the geometry of a molecular cluster is described by $6(n-1)$ intermolecular degrees of freedom, n being the number of molecules which constitute the cluster. Since $n = 2$ in the present case, there are six parameters to characterize the relative position of water to CNA: three coordinates for the center of mass of water with respect to CNA and the rest for their relative orientation. However, there are only four experimental data (rotational constants A and C for CNA–H_2O and CNA–D_2O), which are insufficient to determine all the six structural parameters unequivocally. Therefore, it is assumed here that the water molecule lies in the CNA plane. This assumption reduces the six parameters into three: two translational degrees of freedom and one rotational. This assumption is justified by the results on closely related species, benzonitrile–water, which has been determined to be planar, including the water hydrogens, from FTMW measurements on five isotopomers [2–4,6]. Most hydrates of *N*-heterocyclic aromatics, such as pyrazine [30], pyrimidine [31], and pyridazine [32], have been also determined to be planar (or nearly planar). It is noted that the planarity of the complex conflicts with the results obtained by the present MO calculations at the DFT/B3LYP/6-31G(d, p) level, which predict planar structures as transition states. However, this non-planarity in the calculated structure is spurious because polarization effects are included only insufficiently. It has been shown for pyrimidine–water that the non-bonded hydrogen atom of water is predicted to lie out of the complex plane in the optimized geometry at the 3-21G(d) and 6-31G(d, p) levels, whereas the complex turns out to be nearly planar when a larger 6-31G++(d, p) basis set is adopted [31]. Unfortunately, such an extensive calculation cannot be performed for CNA–water because of its much larger size.

The four experimentally determined rotational constants have been subjected to a least-squares fit to derive three geometrical parameters: the $r(O\cdots N)$ distance, the $r(O\cdots H_1)$ distance, where the 1-position H atom of CNA is denoted here-

after as H_1, and the $\angle H_1OH_b$ angle, where H_b is the water H (or D) atom which participates in the hydrogen bond. The structure of the CNA–water complex derived from the above-mentioned assumption is shown in Fig. 5. The trace simulated for this structure, shown in Fig. 2b, reproduces the experimental one (Fig. 2a) quite well. The geometrical parameters thus obtained are: $r(O\cdots N) = 3.06 \pm 0.01$ Å, $r(O\cdots H_1) = 2.47 \pm 0.01$ Å, and $\angle H_1OH_b = 70 \pm 10°$, where errors represent one standard deviation of the fit. We have assessed the range of possible deviations from the geometry of Fig. 5 retaining the consistency with the RCS-derived rotational constants. We find that displacements of $r(O\cdots N)$ by ± 0.10 Å, $r(O\cdots H_1)$ by ± 0.05 Å, and $\angle H_1OH_b$ by $\pm 40°$ yield structures whose rotational constants are compatible with the measured ones within experimental error.

A least-squares fit has been also made under the assumption that the non-bonded H (or D) atom of water deviates from the plane, thus taking a perpendicular orientation. The results are: $r(O\cdots N) = 3.08 \pm 0.11$ Å, $r(O\cdots H_1) = 2.48 \pm 0.06$ Å, and $\angle H_1OH_b = 120(+60, -30)°$, where uncertainties represent the ranges of possible deviations. The position of the O atom changes little, but $\angle H_1OH_b$ varies considerably and the O–H_b bond is deviated away from the CN group. This orientation of water is inconsistent with the expected hydrogen bonding between CNA and water, excluding the possibility for the (almost) perpendicular conformation.

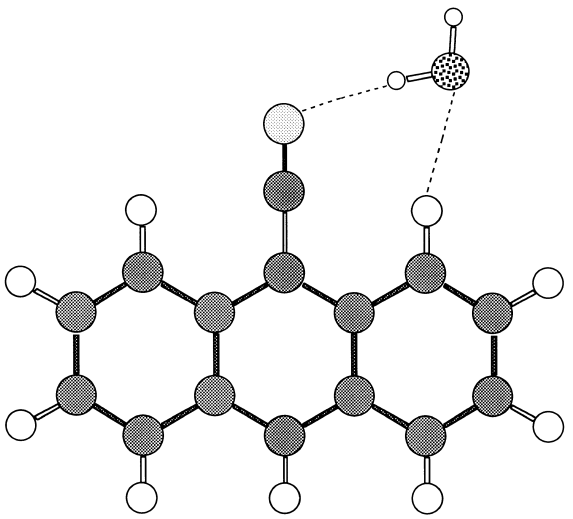

Fig. 5. Geometry of CNA–water determined by a least-squares fit of the RCS-derived rotational constants.

The results from MO calculations at the DFT/B3LYP/6-31G(d, p) level, $r(O\cdots N) = 2.981$ Å, $r(O\cdots H_1) = 2.389$ Å, and $\angle H_1OH_b = 83.66°$, agree reasonably with those derived from experiment. However, note again that the planar structure corresponds to transition states at the present level of calculations. The experimental value of $r(O\cdots N)$, 3.06 ± 0.10 Å, is close to that of benzonitrile–water in the S_0 state, 3.161 Å [6], though the orientation of water with respect to benzonitrile is significantly different from that in CNA–water. This suggests that the hydrogen bonding is local interaction between the polar cyano group and water and is affected only slightly by the aromatic part, either phenyl or anthryl.

The obtained value of $r(O\cdots H_1)$ of CNA–water is also similar to that of benzonitrile–water, 2.484(1) Å [6]. These distances are smaller than a simple sum of the van der Waals radii of H and O atoms (2.72 Å) [33], indicating a significant interaction between the C–H bond and the O atom of water. This interaction also seems to influence the structures of hydrated *N*-heterocyclic aromatics [30–32]. Such C–H$\cdots$O hydrogen bonds have been considered as an important intermolecular interaction, especially by affecting the higher-order structures of biological systems like proteins [34,35].

Finally, we briefly discuss the possible large-amplitude intermolecular motion in the CNA–water complex. The hydrogen atoms of the water molecule can be interconverted through internal rotation, e.g., that around the C_2 symmetry axis. The quantum tunneling motion makes each vibronic state split into two, the lower and upper levels being coupled with the ortho ($I = 0$) and para ($I = 1$) nuclear spin states of hydrogen, respectively. Such interconversion doubling has been observed for benzonitrile–water by FTMW measurements [6], and the potential barrier has been established from the tunneling-state dependence of the determined rotational constants (in the order of 10^{-3}%). In the present case, the resolution of the RCS measurements is not sufficient to resolve the

tunneling splitting in the CNA–water cluster, and much larger upper limit ($\leqslant 0.5\%$) is set for the difference between the rotational constants of the two tunneling states.

5. Conclusion

We have presented the structure of the CNA–water complex by RCS. The gross structure is a side-type, where the water molecule is hydrogen-bonded to the π-electrons of the cyano group of the CNA. Some of the geometrical parameters are derived from the rotational constants obtained from the experimental results of RCS, and a planar structure is suggested. The C–H$\cdots$O hydrogen bonding is identified as one of the important intermolecular interactions which characterize the cluster geometry.

Acknowledgements

The present work has been supported by Grants-in-Aid (Nos. 08454177 and 10440172) from the Ministry of Education, Science, Sports and Culture of Japan. Additional support has been provided from Japan Science and Technology Corporation (JST). Y.O. thanks the Mitsubishi Chemical Foundation, the Japan Securities Scholarship Foundation, and Asahi Glass Foundation for financial support.

References

[1] T. Kobayashi, K. Honma, O. Kajimoto, S. Tsuchiya, J. Chem. Phys. 86 (1987) 1111.
[2] V. Storm, D. Consalvo, H. Dreizler, Z. Naturforsch. 52a (1997) 293.
[3] R.M. Helm, H.-P. Vogel, H.J. Neusser, V. Storm, D. Consalvo, H. Dreizler, Z. Naturforsch. 52a (1997) 655.
[4] V. Storm, H. Dreizler, D. Consalvo, Chem. Phys. 239 (1998) 109.
[5] S. Ishikawa, T. Ebata, N. Mikami, J. Chem. Phys. 110 (1999) 9504.
[6] S. Melandri, D. Consalvo, W. Caminati, P.G. Favero, J. Chem. Phys. 111 (1999) 3874.
[7] R. Yamamoto, S. Ishikawa, T. Ebata, N. Mikami, J. Raman Spectrosc. 31 (2000) 295.
[8] E.M. Gibson, A.C. Jones, A.G. Taylor, W.G. Bouwman, D. Phillips, J. Sandell, J. Phys. Chem. 92 (1988) 5449.
[9] T. Kobayashi, M. Futakami, O. Kajimoto, Chem. Phys. Lett. 130 (1986) 63.
[10] J.A. Warren, E.R. Bernstein, J.I. Seeman, J. Chem. Phys. 88 (1988) 871.
[11] V.H. Grassian, J.A. Warren, E.R. Bernstein, H.V. Secor, J. Chem. Phys. 90 (1989) 3994.
[12] O. Kajimoto, H. Yokoyama, Y. Ooshima, Y. Endo, Chem. Phys. Lett. 179 (1991) 455.
[13] Q.-Y. Shang, E.R. Bernstein, J. Chem. Phys. 97 (1992) 60.
[14] B.D. Howells, J. McCombie, T.F. Palmer, J.P. Simons, A. Walters, J. Chem. Soc. Faraday Trans. 88 (1992) 2603.
[15] K. Fujita, T. Fujiwara, K. Matsunaga, F. Ono, A. Nakajima, H. Watanabe, T. Koguchi, I. Suzuka, H. Matsuzawa, S. Iwata, K. Kaya, J. Phys. Chem. 96 (1992) 10693.
[16] V. Brenner, A. Zehnacker, F. Lahmani, Ph. Millié, J. Phys. Chem. 97 (1993) 10570.
[17] Y. Stepanenko, A. Vdovin, J. Jasny, J. Sepioł, A. Mordziński, J. Mol. Struct. 480–481 (1999) 595.
[18] P.M. Felker, J. Phys. Chem. 96 (1992) 7844.
[19] K. Egashira, Y. Ohshima, O. Kajimoto, J. Phys. Chem. A (in press).
[20] M.J. Côté, J.F. Kauffman, P.G. Smith, J.D. McDonald, J. Chem. Phys. 90 (1989) 2865.
[21] J.F. Kauffman, M.J. Côté, P.G. Smith, J.D. McDonald, J. Chem. Phys. 90 (1989) 2874.
[22] M.J. Frisch et al., GAUSSIAN98, Gaussian, Inc., Pittsburgh PA, 1998.
[23] A. Amirav, C. Horwitz, J. Jortner, J. Chem. Phys. 88 (1988) 3092.
[24] P.M. Felker, A.H. Zewail, J. Chem. Phys. 86 (1987) 2460.
[25] G.V. Hartland, L.L. Connell, P.M. Felker, J. Chem. Phys. 94 (1991) 7649.
[26] P.M. Felker, A.H. Zewail, in: J. Manz, L. Wöste (Eds.), Femtosecond Chemistry, vol. 1, VCH, Weinheim, 1995, (chap. 5).
[27] S. Kato, Y. Amatatsu, J. Chem. Phys. 92 (1990) 7241.
[28] W.S. Benedict, N. Gailar, E.K. Plyler, J. Chem. Phys. 24 (1956) 1139.
[29] R.M. Macfarlane, M.R. Philpott, Chem. Phys. Lett. 41 (1976) 33.
[30] W. Caminati, L.B. Favero, P.G. Favero, A. Maris, S. Melandri, Angew. Chem., Int. Ed. Engl. 37 (1998) 792.
[31] S. Melandri, M.E. Sanz, W. Caminati, P.G. Favero, Z. Kisiel, J. Am. Chem. Soc. 120 (1998) 11504.
[32] W. Caminati, P. Moreschini, P.G. Favero, J. Phys. Chem. A 102 (1998) 8097.
[33] A. Bondi, J. Phys. Chem. 68 (1964) 441.
[34] T. Steiner, W. Saenger, J. Am. Chem. Soc. 115 (1993) 4540.
[35] Z.S. Derewenda, L. Lee, U. Derewenda, J. Mol. Biol. 252 (1995) 248.